# AN INVESTIGATION ON THE DIFFUSER-INDUCED VIBRATION INSTABILITY OF A ROD IN AXIAL ANNULAR FLOW

Heung Seok Kang, Njuki W. Mureithi, and Michel J. Pettigrew
*BWC/AECL/UNSERC Chair of Fluid-Structure Interaction,*
*Department of Mechanical Engineering, Ecole Polytechnique,*
*Box 6079, Station Centre-ville, Montreal, QC, Canada, H3C 3A7*

## ABSTRACT

*Significant research has been done on the annular-flow-induced vibration of a concentric centerbody commonly found in reactor internals. In order to utilize the research results for heat exchanger tubes, however, the practical conditions provided by the tube-support plate geometry should be considered. With heat exchanger tubes, the support causes leakage flow (very confined annular flow) and sometimes, additional divergent or convergent flow at the exit or the entrance of the support, which is due to chamfering of the support hole for manufacturing convenience. Therefore, when it comes to heat exchangers, leakage flow over a finite length and divergent or convergent fluid boundary conditions should be considered in addition to the basic annular flow.*

*In this paper, an analytical as well as experimental approach is taken to investigate i) the instability mechanism, ii) the effects of diffuser parameters such as gap (leakage) size and diffuser angle on the instability and iii) develop an analytical model for the rod subjected mostly to annular flow and leakage and divergence flow through a finite-length diffuser at the middle of the rod.*

*It is found by experiment and theoretical model that the tube loses stability by flutter at very low flow velocity.*

## 1. INTRODUCTION

Considerable effort has been made to develop methodologies to predict instabilities on annular- or leakage-flow-induced vibration of a flexible rod. AS a result, several methods to predict the dynamic behavior have been developed, such as the linearized potential flow theory (Mateescu, Paidoussis and Sim, 1985, 1987, 1988), and the pressure-loss models (Hobson, 1982; Spurr and Hobson, 1984; Fujita and Ito, 1992; Langthjem et al., 2006). The basic dynamics due to annular flow are known by virtue of these models. On the other hand, to tackle industrial problems such as heat exchanger tube and control rod vibrations in gas and water cooled reactors, practical conditions must be considered. These include finite-length gap supports, much smaller gap resulting in leakage flow and convergent or divergent boundary conditions at the entrance and the exit of the support.

Unlike the basic annular flow case, a rigid rod translating periodically in a finite length annular region of confined flow was studied by Mulcahy (1980). He studied the fluid forces and hydraulic damping. However, since the study was only done for still water, only positive damping was found. Later, Yasuo and Paidoussis (1989) tried to solve the flow-induced instability problem of heat exchanger tubes subjected to axial flow in a diffuser-shaped, loose intermediate support which is the same problem as this study tries to solve. In their study, potential flow theory was considered with a one-mode approximation of the inner tube. They suggested a critical flow velocity equation either for divergence and flutter. Application of this theory to real problems is, however, limited because of the one-mode approximation and unrealistic prediction of the critical flow velocity.

## 2. EXPERIMENT

### 2.1 Description of apparatus

Experiments were conducted in a 2.5m long test section in which the flow rate ranged from 3 to 50 SCFM (Standard Cubic Feet per Minute). A 2.2 m long and 15.9 mm (0.627 inch) diameter inner tube was used with several mid-supports (finite-length diffusers) having a length of 38.7 mm (1.525 inch). The inner tube was supported by four pins at one end, therefore, a total of eight points for both ends to simulate pinned-pinned boundary conditions. The gaps between the inner tube and supports were 0.3 mm, 0.4 mm and 0.66 mm, and the annular gap between the inner tube and outer plastic glass tube is 5.0 mm. Vibration amplitudes were measured with four laser sensors in two directions near the supports at mid span and at one-fourth position along the test section. The measured voltage signals

were gathered through a data acquisition system and analyzed with a Oros signal analysis system. Figure 1 shows basic the test setup.

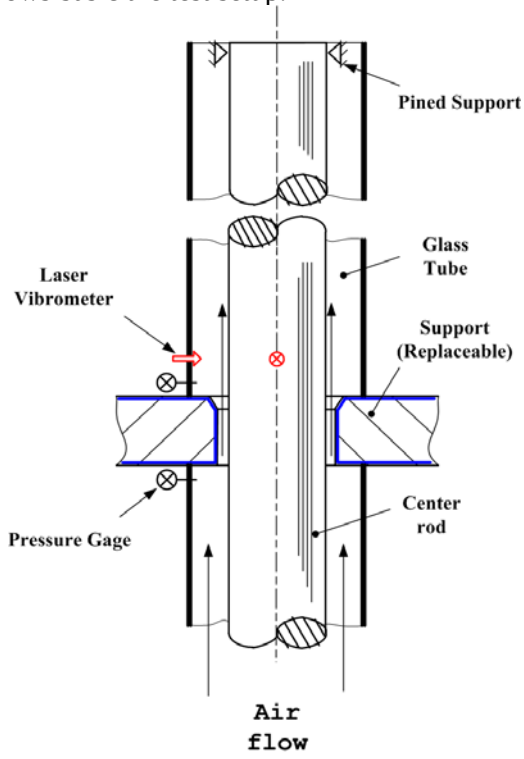


Figure 1*: Sketch of experimental apparatus*

## 2.2 Experimental results

Figure 2 shows the measured vibration amplitudes for supports having 0.4, 0.66 and 2.2 mm gap with a 10° diffuser angle. The reference flow velocity is the immediately upstream of the support. The inner pinned-pinned tube loses its first mode stability at very low flow velocity for all three cases. The first instability is clearly shown at the first mode, then, interestingly the third mode instability occurs earlier than the second mode one in Figure 2(c) or at almost the same velocity in Figure 2(b). It is, however, difficult to identify the mode correspond to the second instability from Figure 2(a) and 2(b). For small gaps, there is severe impacting during the first instability by which dynamic energy is possibly dissipated, and the second instability may not be observed. It is believed that the first critical flow velocities for the smaller gaps 0.3 mm and 0.66 mm occur less than 1 m/s while for the largest gap of 2.2 mm, the critical velocity greater than 2 m/s.

The amplitudes for different diffuser angles as functions of flow velocity are shown in Figure 3. From Figure 3 (a, b) and Figure 2 (a. b), we may conclude that the critical flow velocity of the rod in the smallest gap (0.3 mm) is higher than that of the rod in the larger gap (0.4mm) and even much larger in the gap (0.66 mm). Instabilities at higher modes are much more clearly observed for the larger diffuser angles. The first critical flow velocity of the tube with 0.4 mm gap and 20° diffuser angle is less than 1 m/s (≈0.6 m/s), and with 0.66 mm gap and 30° diffuser angle is approximately 1.0 m/s. Instability in the second mode, however, was not of the same order even for the same angle of 20°. The 0.3 mm diffuser, Figure 3(a), loses stability at 3 m/s while the 0.4 mm diffuser, Figure 3(b), destabilizes at 7 m/s.

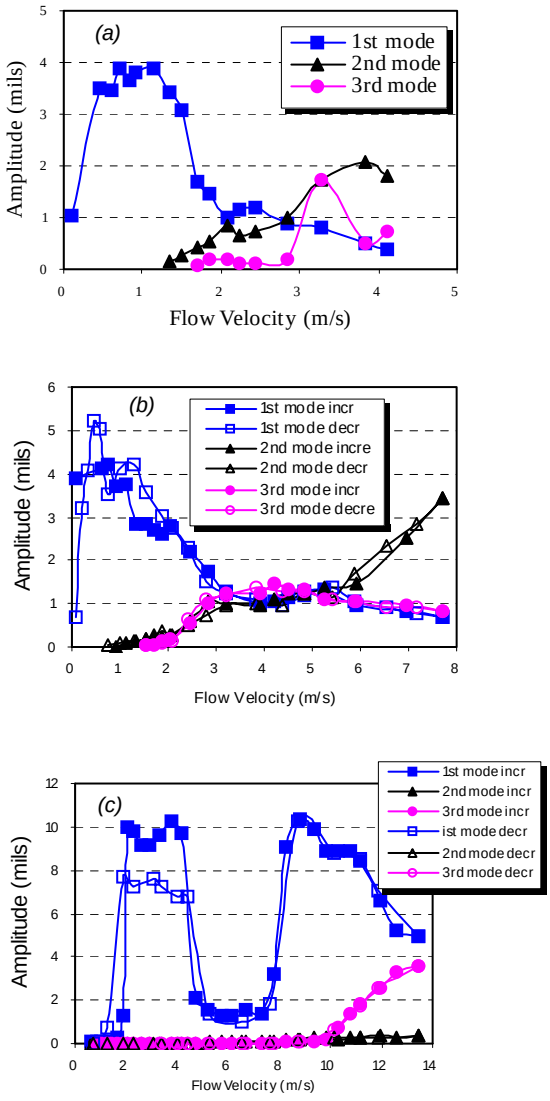


Figure 2*: Vibration response amplitude variation with flow velocity for a 10 ° diffuser and support gap of (a) 0.3 mm, (b) 0.66 mm and (c) 2.2 mm*

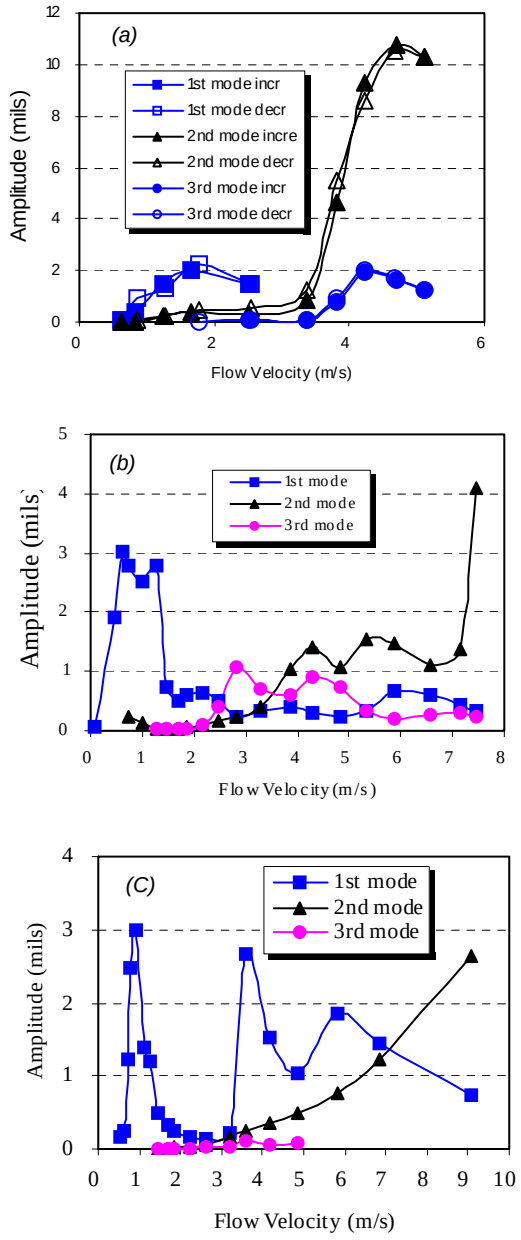


Figure 3: *Vibration response amplitude variation with flow velocity for a support gap of (a) 0.3 mm /20° angle, (b) 0.4 mm / 20° angle and (c) 0.66 mm / and 30°*

Figure 4 shows X-Y plots of the tube in the plane of the inner tube cross section which corresponds to Figure 2(a). Limit cycles are clearly observed in the flow velocity range of 0.5 m/s to 1.5 m/s, from when the amplitude start to increase sharply to when the amplitude decreases significantly where mild impact starts as shown in Figure 4(b).

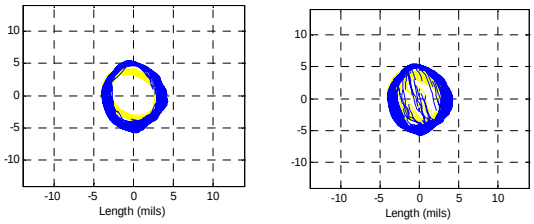


*(a) 1.3 m/s* *(b) 1.5 m/s*

Figure 4: *Trajectories of the inner rod from 0.3 mm gap and 10° diffuser angle*

## 3. THEORETICAL MODEL

### 3.1 General formulation

The system under consideration consists of a basic annulus of constant height, H, much confined annulus of height, G, and small length of diffuser, $L_\alpha$, at a small finite-length of gap support. Detailed parameters are shown in Figure 4.

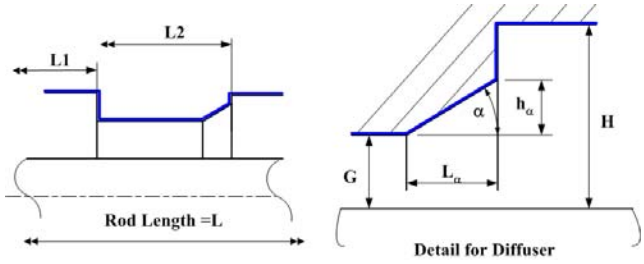


Figure 5*: Dimension of diffuser*

The inner cylinder can vibrate in any mode shape, but in a beam-bending sense, with small amplitude. Based on test results showing that the critical flow velocity is very low compared to the basic annular flow cases, one is inclined to conclude that something happens at the support. In order to develop a theoretical model, therefore, flow perturbations are assumed only to be at the support. For this reason, before and after the support, the equation of motion of the flexible center body may be expressed as follows:

$$EI\frac{\partial^4 h}{\partial x^4}+2M_f U\frac{\partial^2 h}{\partial x\partial t}+M_f U^2\frac{\partial^2 h}{\partial x^2}+C\frac{\partial h}{\partial t}+(M_f+m)\frac{\partial^2 h}{\partial t^2}=0 \qquad (1)$$

The equation of motion at the support may be expressed as follows:

$$EI\frac{\partial^4 h}{\partial x^4}+2M_f U\frac{\partial^2 h}{\partial x\partial t}+M_f U^2\frac{\partial^2 h}{\partial x^2}+C\frac{\partial h}{\partial t}+(M_f+m)\frac{\partial^2 h}{\partial t^2}=F_f \qquad (2)$$

$F_f$ means an additional forcing function induced by the fluid at the support. By assuming perturbation of every terms in equation (2), and introducing dimensionless parameters as follows,

$$x = \frac{x^*}{L^*},\ h = \frac{h^*}{a^*},\ H = \frac{H^*}{a^*},\ P = \frac{P^*}{\rho U^{*^2}},\ u = \frac{u^*}{U^*},$$

$$U = \left(\frac{M_f}{EI}\right)^{1/2} L^* U^*,\quad t = \left(\frac{EI}{M_f + m}\right)^{1/2} \frac{t^*}{L^{*^2}},$$

$$\beta = M_f/(M_f + m), \tag{3}$$

$$\sigma = \frac{CL^{*^2}}{\left[EI\left(M_f + m\right)\right]^{1/2}},\ \omega = \left(\frac{M_f + m}{EI}\right)^{1/2} \Omega L^{*^2}$$

the nondimensional form of equation of motion may be expressed as

$$\frac{\partial^4 h}{\partial x^4} + 2\beta^{1/2}\bar{U}\frac{\partial^2 h}{\partial x \partial t} + \bar{U}^2\frac{\partial^2 h}{\partial x^2} + \sigma\frac{\partial h}{\partial t} + \frac{\partial^2 h}{\partial t^2} = Q\cdot(-p_f) \tag{4}$$

where $p_f$ and Q in equation (4) are respectively pressure and a constant left by nondimensionlization. The pressure $p_f$ in equation (4) may be expressed by

$$p_f = \lambda^2 p_i + \lambda p_d + p_k \tag{5}$$

Once the perturbation pressure ( $p_f$ ) is obtained, Galerkin's method may be utilized. The basic equation for the Ritz criterion is possibly separated into three parts; before the support, at the support and after the support.

$$\int_0^L \varphi_j \varepsilon(\varphi_i)dx = 0$$

$$\int_0^{L1} \varphi_j \varepsilon(\varphi_i)dx + \underbrace{\int_{L1}^{L2} \varphi_j \varepsilon(\varphi_i)dx}_{\text{support}} + \int_{L2}^{1} \varphi_j \varepsilon(\varphi_i)dx = 0 \tag{6}$$

### 3.2 Equation of fluid motion

To derive the fluid equations at the support, several assumptions are made as follows:

(*i*) the fluid is incompressible,

(ii) transverse components are neglected, hence one dimensional flow,

(iii) static pressure is recovered at the exit of the support.

(iv) flow perturbation exists only at the support.

Linearization of the 1-D continuity and momentum equations is utilized to obtain the expression of the fluctuating velocity and pressure. Then, the three fluid force terms in equation (5), inertial, damping and stiffness terms, are identified.

The 1-D continuity and momentum equations for an incompressible fluid may be expressed as

$$\frac{\partial H}{\partial t} + \frac{\partial}{\partial x}(HU) = 0 \tag{7}$$

$$\rho\frac{\partial}{\partial t}(HU) + \frac{\partial}{\partial x}\left[H\left(P + \rho U^2\right)\right] - P\frac{\partial H}{\partial x} + 2\tau_x = 0 \tag{8}$$

The friction term may be expressed as

$$\tau = \tau_{S.f} + \tau_{p.f} = \frac{1}{2}C_f \rho U^2 + C_f \rho U u \tag{9}$$

Considering perturbation of every parameters and dimensionless parameters in equation (3), the following linearlized fluid perturbation equations are obtained.

$$\beta^{1/2}\frac{\partial h}{\partial t} + U\frac{\partial h}{\partial x} + HU\frac{\partial u}{\partial x} = 0 \tag{10}$$

$$PU\frac{\partial p}{\partial x} + \beta^{1/2}\frac{\partial u}{\partial t} + U\frac{\partial u}{\partial x} + 2\cdot C_f\frac{l_s}{\bar{H}}Uu = 0 \tag{11}$$

Applying Bernoulli's equation at the support entrance, where the flow passage is contracted, one arrives at the following boundary condition in dimensionless form,

$$p_{in} + u_{in}(1 + K_c) = 0 \tag{12}$$

A diffuser efficiency, $\bar{\eta}$, may be defined in terms of the static pressure recovered in steady flow as follows:.

$$\bar{p}_{ex} - \bar{p}_{spt} = \bar{\eta}\cdot\frac{1}{2}\rho\bar{u}_{spt}^2 \tag{13}$$

Every term in equation (13) may be considered as consisting of static and dynamic components. As in the previous treatment, then, equation (13) can be linearized. It may be assumed that the dynamic diffuser efficiency $\eta$ is a function of the area ratio or the diffuser angle $\alpha$ so that

$$\bar{\eta}(\alpha, t) = N_e + \eta(\alpha, t) \tag{14}$$

$$\eta(\alpha, t) = \frac{dN_e}{dg(\alpha)}\cdot h(t) \tag{15}$$

At the diffuser section, $g = G + h_\alpha$ , therefore,

$$dg = dh_\alpha \tag{16}$$

Using a definition similar to Hobson's (1982) for the performance coefficient δ we have

$$\delta = \frac{dN_e}{dg(\alpha)/G}. \tag{17}$$

The dimensionless diffuser performance coefficient in equation (17) does not have the identical definition to Hobson's, but it is closely similar.

Equation (13) can be divided into steady and perturbation terms as follows.

$$P_{ex} - P_{spt} = \mathrm{N}_e \cdot \tfrac{1}{2}\rho U_{spt} \tag{18}$$

$$p_{ex} - p_{spt} = \mathrm{N}_e \cdot \rho U_{spt} u_{spt} + \tfrac{h}{G}(\delta)\tfrac{1}{2}\rho U_{spt}^2 \tag{19}$$

The static diffuser efficiency ($N_e$) can be determined by equation (18) while $h_\alpha$ may be expressed as $h_\alpha = L_\alpha \alpha$, so equation (16) becomes

$$dg = dh_\alpha = L_\alpha d(\alpha) \tag{20}$$

Substituting equation (20) into equation (17), gives

$$\delta = \frac{1}{L_\alpha / G} \cdot \frac{dN_e}{d\alpha} \tag{21}$$

In equation (19), $p_{ex}$ assumed to be zero.

Now, the fluid equation (10) and (11) can be solved with the two boundary conditions, (12) and (19) and pinned-pinned beam eigenfunctions:

$$h_i = \sqrt{2} \cdot Sin\left[\lambda r_i \cdot x\right] \cdot e^{\lambda t} \tag{22}$$

The eigenfunction is needed here because Galerkin's method is utilized to solve the equations. We have a solution form as follows:

$$p_f = \frac{\lambda^3 P_c(h) + \lambda^2 P_i(h) + \lambda P_d(h) + P_k(h)}{-2C_f L_{spt} l_d U + G\left[(1 + K_c - N_e)U - \lambda \beta^{1/2} L_{spt}\right]} \tag{23}$$

where, *p(h)* means the function of the beam vibration amplitude, *h*, $h(x,t) = \phi(x) \cdot e^{\lambda t}$, and $L_{spt}$ is the length of the support.

Now, substituting equation (23) into equation (4), multiplying the left side of equation (4) by the denominator of equation (23), and then, moving the numerator of the right side to the left side, one may have a third-order equation of motion.

### 3.3 Eigenvalue problem of the third-order system

The basic equation may be written

$$[M_3]\dddot{x} + [M_2]\ddot{x} + [C]\dot{x} + [k]x = 0 \tag{24}$$

Let, $y_1 = x,\ y_2 = \dot{y}_1,\ y_3 = \dot{y}_2$ (25)

Then, three ordinary differential equations are obtained as follows:

$$[M_3]\dot{y}_3 + [M_2]y_3 + [C]y_2 + [k]y_1 = 0 \tag{26-1}$$

$$\begin{aligned} \dot{y}_2 &= [I]y_3 \\ \dot{y}_1 &= [I]y_2 \end{aligned} \tag{26-2}$$

From equation (26), one may constitute a 3×3 state-space matrix formulation.

### 3.4 Application to experimental cases

The pressure recovery efficiency of the supports is obtained by experiment. As shown in Figure 1, the static pressure is not measured at the support, but predicted based on the pressure measurement just prior to the support, flow area ratio, and then friction coefficient predicted as a function of gap flow velocity. Some of the recovery factors seem not to be realistic. It is believed that friction at the support is overestimated or underestimated sometime. Accordingly, the estimated pressure might be lower or higher than the real value, so that the pressure recovery could be evaluated to be high or low. Basically, it is found that the smaller the gap size and the diffuser angle are, the higher the diffuser efficiency.

When the nodal point of the second beam mode, the midpoint of the beam, is in the support somewhere at the straight hole section, then, the rod loses stability by flutter in the first mode near 0.03 – 0.15 dimensionless velocity which is equivalent to 3 – 18 m/s upstream of the glass tube as annular gap size increases from 0.3 mm to 2.2 mm. The critical flow velocity is proportional to the gap size and the diffuser angle. After the first instability, the tube becomes unstable again by flutter at the third mode just after the first. Figure 6 is an Argand diagram for the tube with the gap of 0.3 mm and diffuser angle of 10 degree which shows the inner tube loses stability consecutively by flutter starting from the first mode, then third mode, second mode, and finally fourth mode.

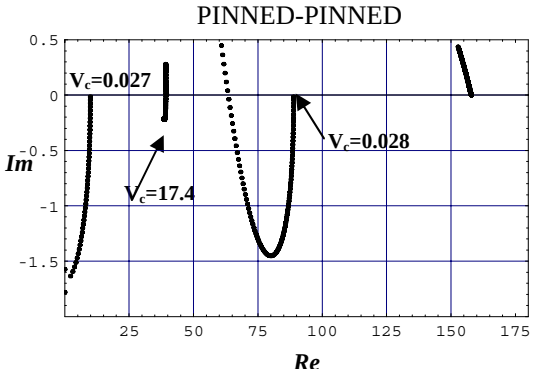


Figure 6: *Argand diagram for 0.3 mm gap and 10 deg. diffuser angle*

One interesting fact is that, when the nodal point of the second mode (midpoint of the rod) is positioned just downstream of the diffuser, the tube loses its stability consecutively by flutter starting

from the first mode, then third mode, fourth mode, and finally second mode, which is shown in Figure 7. All critical flow velocities are below 0.126 (equivalent to 14.5 m/s) for 0.3mm gap/10 deg. diffuser.

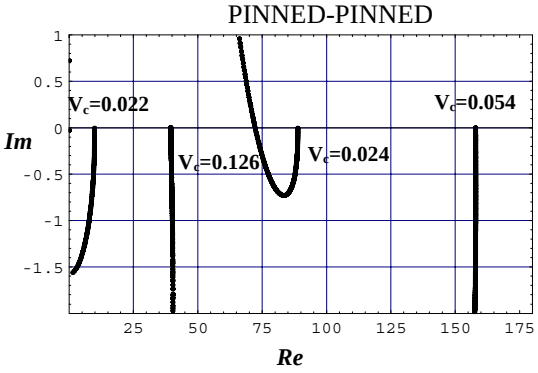


Figure 7: *Argand diagram for 0.3 mm gap and 10 deg. diffuser angle*

## 4. CONCLUSION

Instability of a pinned-pinned flexible rod subjected to mostly annular flow and very tight annular (leakage) flow over a finite-length gap support is studied by theoretical model as well as experiment. Contraction and diffuser boundary conditions at the gap support are considered.

In experiments with a 2.2 m long steel tube, 4 cm support, and moderate air flow, flutter instability is observed for all supports; no matter how large gap sizes or diffuser angles are. With annular flow, the simply supported beam is known to lose stability by divergence at very high flow velocity beyond practical engineering application. A small support interestingly plays a significant role to change the dynamic behavior of the pinned-pinned rod, and additionally, to decrease the critical flow velocities down to engineering flow velocities. The critical flow velocity obtained by the experiment is lower than practical flow velocity generally used in power generation plants.

By analytical approach, a theoretical model has been developed based on small perturbation assumption and 1-D fluid approximation. Numerical simulation for the experimental cases yields the same results as experiment; the rod loses stability by flutter at the first mode, and the critical flow velocity is predicted to be reasonably low (2.5 to 15.5 m/s). The predictions are, however, higher than the measured values. That is possibly due to inaccurate pressure loss estimation and diffuser performance factors.

It is worth noting that the second instability occurs at the third mode, not at the second mode which was observed in some of experiments. When the diffuser of the support is positioned at the nodal point of the second mode, the tube loses stability consecutively by flutter. All critical flow velocities turn out to be well within the range of practical engineering flow velocities.

## 5. REFERENCES


Mateescu, D. and Paidoussis, M.P, 1985, The unsteady potential flow in axially variable annulus and its effect on the dynamics of oscillating rigid centre-body, *J. of Fluid Engineering*, **107**, 421-427.

Mateescu, D. and Paidoussis, M.P, 1987, Unsteady viscous effects on the annular-flow-induced instabilities of rigid cylindrical body in narrow duct, *J. of Fluids and Structures*, **1**, 197-215.

Mateescu, D., Paidoussis, M.P and Sim, W. G., 1988, Dynamics and Stability if a flexible cylinder in a narrow coaxial cylindrical duct, subjected to annular flow, *International Symposium on Flow-Induced Vibration and Noise*, ASME, Nov. 27-Dec. 2. 125-145 Chicago, Illinois.

Hobson, D.E., 1982, Fluid-elastic instabilities caused by flow in an annulus, pp. 440-460, *Proceeding of BNES, 3rd international conference on vibration in nuclear plant*, 440-460. Keswick, U.K.

Spurr, A. and Hobson, D.E., 1984, Forces on the vibrating centerbody of an annular diffuser, *Symposium on Flow-induced Vibration*, ASME, **4**, 41-52.

Fujita, K and Ito, T., 1992, Study of leakage-flow-induced vibration of an axisymmetric cylindrical rod due to axial flow, S*ymposium on Flow-Induced Vibration and Noise*, ASME. PVP **244**, 33-43.

Langthjem, M. A., Morita, H. Nakamura, T. and Nakano, M., 2006, A flexible rod in annular leakage flow: Influence of turbulence and equilibrium offset, and analysis of instability mechanism, *J. of Fluids and Structures*, **22** 617-645.

Mulcahy, T.M., 1980, Fluid forces on rods vibrating in finite length annular regions, *J. of applied mechanics*, **47**, 234-240.

Yasuo, A. and Paidoussis, M. P., 1989, Flow-Induced Instability of Heat-Exchanger Tubes due to Axial flow in a Diffuser-shaped, Loose Intermediate Support, *J. of Pressure Vessel Technology*, **111**, 428-434.